CHAPTER 29

Echocardiographic Assessment of Functional Single Ventricles after the Fontan Operation

Marc Gewillig[1] and Luc L. Mertens[2]

[1] University Hospitals Leuven, Leuven, Belgium

[2] The Hospital for Sick Children; University of Toronto, Toronto, ON, Canada

Introduction

For the majority of patients with different types of functionally univentricular hearts, the treatment goal is to achieve palliation through the creation of a total cavopulmonary connection known as the Fontan operation. This operation essentially bypasses the right heart by redirecting the systemic venous return directly into the pulmonary circulation without passing through a ventricular chamber. The Fontan operation creates a unique circulatory physiology, which resulted in improved survival at the expense of long-term complications. Evaluating a Fontan patient requires a specific echocardiographic approach and careful interpretation of the findings. In this chapter we first review the physiologic characteristics of a Fontan circulation followed by a discussion of the echocardiographic evaluation.

The Fontan circulation

A Fontan circulation is offered to patients with severe congenital heart disease who have only one functional single ventricle (FSV) or those in whom the ventricular cavity cannot be partitioned into two adequate pumps. During fetal life and immediately after birth, the systemic and the pulmonary circulations in an FSV are connected in parallel with one ventricular chamber pumping to both circulations (Figure 29.1). Initially these patients are palliated by an aortopulmonary artery shunt (e.g., a Blalock–Taussig shunt or ductal stent), right ventricular (RV) to pulmonary artery (PA) shunt (also termed a Sano-type shunt), or by PA banding. All these procedures result in persistence of the parallel circulations with mixing of saturated and desaturated blood causing arterial desaturation as well as chronic volume loading of the FSV. In the pre-Fontan era this was the only type of palliation that could be offered, often requiring upscaling the shunts or loosening the PA band. These procedures were associated with progressive ventricular dysfunction, heart failure, progressive desaturation, and death, with few survivors beyond the fourth decade. In 1971, Francis Fontan, a cardiac surgeon in Bordeaux, France, reported on a novel surgical approach to single ventricles [1], separating the systemic and pulmonary circulations by redirecting the systemic venous blood directly to the pulmonary circulation. In the Fontan circulation, mixing of the circulations is abolished and the postcapillary energy and systemic venous pressure are used as the driving forces to propel the blood through the pulmonary circulation [2]. Advantages of a Fontan circuit include separation of both circulations with normalization of the arterial saturation and significant ventricular volume unloading [3,4]. Initially, different types of connections were used to redirect the systemic venous blood to the pulmonary circulation; however the Fontan operation has been simplified by connecting the caval veins directly to the pulmonary arteries. This is achieved by first performing a bidirectional Glenn shunt by direct anastomosis of the superior vena cava to the pulmonary artery and in a second stage by connecting the inferior vena cava through an intra- or extracardiac conduit to the pulmonary artery. A modern Fontan operation is thus an extracardiac operation. The early changes observed at ventricular level are not related to cardiac surgery but are secondary adaptations to the new physiologic stage. After Fontan surgery an additional upstream flow restrictor determines the inflow to the FSV as, by creating a Fontan circuit, the pulmonary circulation is positioned, like a portal system, between the systemic venous return and the systemic ventricle. A portal system is defined as a capillary network that is interposed between another capillary network and the heart. This pulmonary portal system now functions like a dam in the cardiovascular circuit, resulting in upstream congestion and reduced downstream flow. The upstream energy is used to push blood through the pulmonary circulation, which provides systemic oxygenation. The pulmonary circulation thus becomes the main limiting factor in the circulation. This results in pooling of systemic venous blood, increased systemic venous pressure, and reduced cardiac output, which

Echocardiography in Pediatric and Congenital Heart Disease: From Fetus to Adult, Third Edition. Edited by Wyman W. Lai, Luc L. Mertens, Meryl S. Cohen and Tal Geva.

Companion website: www.wiley.com/go/lai-echo3

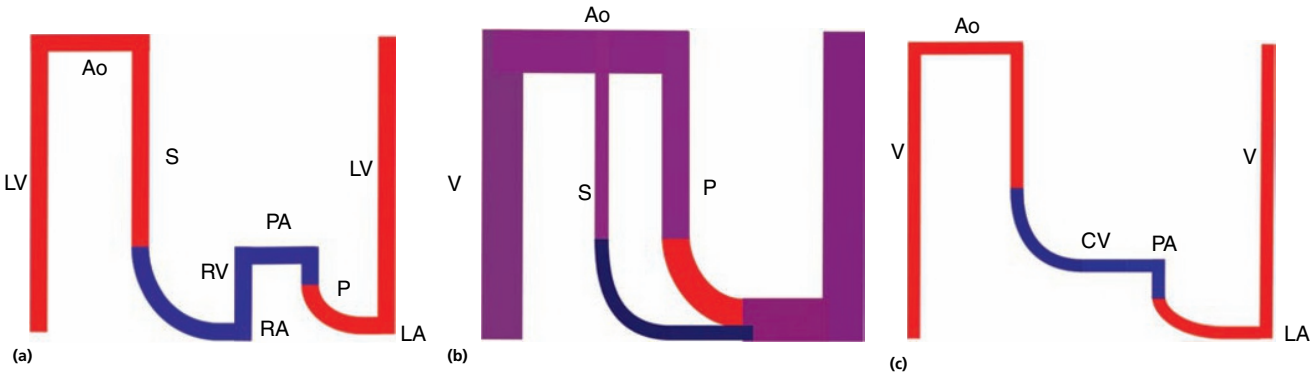

Figure 29.1 Schematic representation of the normal cardiovascular circulation **(a)**, shunted palliation **(b)**, and Fontan circulation **(c)**. **(a)** The normal circulation. The pulmonary circulation (P) is connected in series with the systemic circulation (S). The right ventricle (RV) is more compliant than the left ventricle (LV), keeping the right atrial (RA) pressure lower than the left atrial (LA) pressure. The RV functions at lower pressure than the LV which is related to lower pressure and resistance in the pulmonary artery (PA). **(b)** Parallel circulation in a univentricular heart. The systemic (S) and pulmonary (P) circuits are connected in parallel with one dominant single ventricle (V) pumping blood into both circulations. There is complete admixture of systemic and pulmonary venous blood, causing arterial desaturation. **(c)** Fontan circuit. The caval veins (CV) are connected to the PA, without a subpulmonary ventricle or systemic atrium: the lungs are hereby converted into a portal system which limits flow to the ventricle. In the absence of a fenestration, there is no admixture of systemic and pulmonary venous blood, but the systemic venous pressures are generally elevated. Ao: aorta. Line thickness reflects output; color reflects oxygen saturation.

are the basis for the most frequent early and late complications of the Fontan circuit (Figure 29.2).

The optimal Fontan circuit requires unobstructed Fontan connections, good-sized branch PAs without stenosis, low pulmonary vascular resistance (PVR), unobstructed pulmonary venous connections to the atrium, and low atrial pressures. Atrial pressures are influenced by atrioventricular (AV) valve function and by FSV diastolic function. Good systolic FSV function is required to generate sufficient systemic output. Chronic volume loading caused by residual shunts, AV valve regurgitation, or aortic regurgitation and/or pressure loading related to outflow tract obstruction, residual coarctation of the aorta, or arterial hypertension can be detrimental in patients after Fontan surgery.

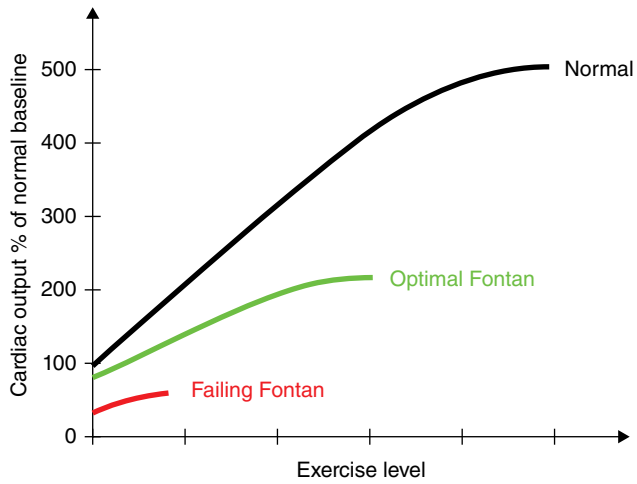

Figure 29.2 Cardiac output during exercise: normal versus Fontan circulation. A normal subject with a biventricular circuit can increase output five-fold compared to baseline (black line). In Fontan patients output is significantly impaired both at rest and during exercise. In optimal Fontan patients (green line) the output is mildly decreased at rest, with a moderately reduced capacity to increase cardiac output during exercise. This limits exercise capacity in almost all Fontan patients. In failing Fontan patients (red line), the output is significantly reduced at rest with very limited increase during exercise.

Functional single ventricle in a Fontan circulation

Ventricular dimensions and wall thickness

The FSV volume load evolves from excessive during fetal life and initial palliation to chronic deprivation after creation of the cavopulmonary shunts (Figure 29.3). During fetal life, the dominant ventricle provides the combined output of the systemic and pulmonary circulations. This causes prenatal eccentric remodeling that results in enlarged chamber dimensions of the FSV at birth (large for body surface area (BSA)) [5]. After the initial neonatal palliation (generally an aortopulmonary artery shunt or a PA band), the parallel circulations cause a persistent, chronic volume loading. Between 4 and 8 months of age, the next step typically consists of dividing the initial shunt (which will normalize the preload for BSA) and creating a bidirectional Glenn shunt (a superior cavopulmonary anastomosis where only the superior vena cava is connected to the PA and the inferior vena cava remains connected to the right atrium), which reduces the pulmonary flow. A serial follow-up study using cardiac MRI in patients scanned before the bidirectional Glenn shunt and again before the Fontan operation demonstrated that the bidirectional Glenn shunt resulted in a reduction of indexed ventricular volume with an increase in

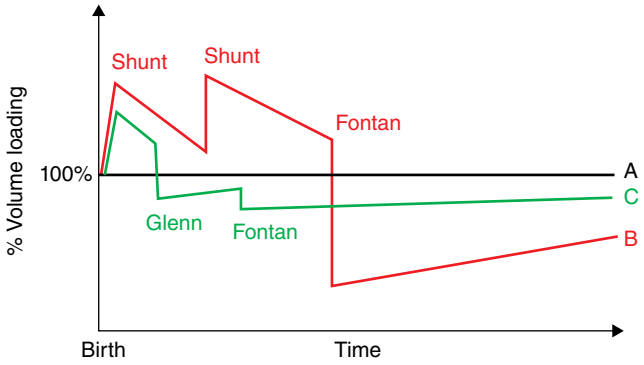

Figure 29.3 Effect of different pre-Fontan palliative strategies on volume loading. A: We assume a normal ventricle in a biventricular circulation functions on average at 100% of normal. Prior to birth the dominant single ventricle remodels and its size adjusts to the chronic volume loading. The patient with a univentricular heart generally is born with an appropriate ventricular size adjusted for chronic volume load. Prior to the 1990s (B, red line), the volume loading to the ventricle was augmented shortly after birth by a shunt procedure to ± 150%. The patient slowly outgrew the shunt, and the ventricle adapted, thereby gradually reducing the volume overload to ± 100% for its size. A second shunt was created, augmenting the volume overload again to 150%. As the patient again outgrew the shunt, a Fontan circuit was made, all of a sudden reducing the volume load to around 25% of the preload it was exposed to prior to the procedure. This sudden preload reduction was often poorly tolerated hemodynamically. This resulted in changes in management strategy. After the 1990s (C, green line), a small neonatal shunt is created for a short time (generally 6 months); the patient slowly outgrows the shunt; the ventricle is progressively volume unloaded in two separate steps: first at the time of the bidirectional Glenn shunt and a second time at the time of the Fontan operation. This stepwise approach is generally hemodynamically better tolerated.

ejection fraction (i.e., reverse remodeling) [6]. Quantitative measurements by cardiac MRI have also demonstrated that flow through aortopulmonary collaterals may contribute significantly to pulmonary blood flow and cardiac output after the bidirectional Glenn shunt [7]: up to one-third of the cardiac output and up to 40% of the pulmonary blood flow comes from collateral flow. A higher burden of collateral flow adversely influences clinical outcomes immediately after the Fontan operation [7,8]. Despite the presence of collaterals, the FSV is further volume unloaded after the Fontan completion by damming off the inferior caval flow. After the Fontan operation, further reverse remodeling of the FSV occurs, characterized by a decrease in ventricular volume with persistence of an abnormal wall thickness (eccentric remodeling) and resulting in increased mass-to-volume ratio [9]. Concentric hypertrophy may also develop in the FSV in response to increased afterload, defined as ventricular wall stress. Studies have suggested that increased afterload (i.e., outflow tract obstruction, residual coarctation of the aorta, or systemic hypertension) may persist or develop after the Fontan operation [10,11]. Residual ventricular hypertrophy may contribute to diastolic dysfunction and eventually to failure of the Fontan circulation.

Effect of loading changes on parameters of systolic function

The most commonly used parameter to assess global pump function is ejection fraction. This parameter is sensitive to changes in preload and afterload. Serial data obtained with either MRI or echocardiography have demonstrated a decrease in ventricular volumes and ejection fraction immediately after the bidirectional Glenn shunt [6,12]. During the remodeling process a compensatory decrease in end-systolic volumes may result in an increase in ejection fraction just prior to the Fontan procedure [6]. Despite these findings, ejection fraction is generally preserved in the majority of patients after the Fontan operation suggesting that adaptation or further reverse remodeling occurs in the post-Fontan period [9]. It also indicates that systolic dysfunction is uncommon in pediatric Fontan survivors. In contrast, in adult patients, ventricular dysfunction seems to be more common and contributes to the failure of the Fontan circuit [13]. Systolic dysfunction may be intrinsic to the FSV or may be related to other comorbidities in adult life.

Diastolic function of the functional single ventricle

In the Fontan circuit, low atrial pressure is required for a low gradient across the pulmonary vascular bed (transpulmonary gradient). AV valve regurgitation and FSV diastolic function are important determinants of atrial pressure. Diastolic function after the Fontan operation has been poorly studied due to the absence of good methods for assessment of ventricular filling in patients with this physiology. Experimental data have shown that acute volume unloading of the ventricle results in less recoil and decreased suction, resulting in increased filling pressures (Figure 29.4) [14]. Echocardiographic studies in Fontan patients

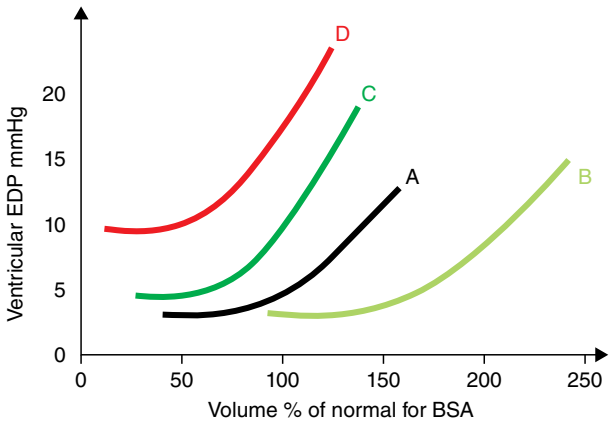

Figure 29.4 Diastolic pressure–volume relationship during different stages of palliation. A: The normal ventricle. B: Shunted ventricle with chronic volume loading resulting in enhanced compliance. C: Fontan ventricle early after volume unloading. D: Fontan ventricle late after unloading: chronic volume unloading is thought to cause progressive stiffening of the ventricle with decreased compliance. BSA, body surface area; EDP, end-diastolic pressure.

have suggested that the volume reduction associated with the Fontan operation results in early relaxation abnormalities and incoordinate wall motion abnormalities especially affecting the isovolumetric relaxation period and early filling [15–17]. These diastolic changes have typically been observed in FSV patients who underwent a Fontan operation without a previous bidirectional Glenn shunt. In this era, the chronically volume-loaded ventricles were acutely unloaded and the observed diastolic and systolic abnormalities could be related to the ventricle being "too large" for the volume immediately after the procedure. In patients after the Fontan procedure, chronic volume reduction with absence of exercise-induced ventricular stretch seems to cause a progressive decrease in ventricular compliance with a left and upward shift in the end-diastolic pressure–volume relationship. It can be expected that the thicker myocardium may become stiffer with age. The FSV may enter a vicious circle whereby the volume unloading results in adverse reverse remodeling, reduced compliance, and reduced ventricular filling, further limiting cardiac output and increasing systemic venous pressures. A cohort study suggested that the majority of pediatric Fontan patients have abnormal diastolic parameters on echocardiography but the clinical and prognostic significance of these findings is currently unknown [9]. The main issue regarding assessment of diastolic function is that the conventional echocardiographic parameters (AV valve inflow, pulmonary venous flow patterns, and tissue Doppler velocities) are difficult to interpret in Fontan patients with a deprived preload. It is difficult to determine whether the observed changes in diastolic functional parameters are related to intrinsic myocardial diastolic dysfunction or are secondary to volume unloading. Typically, diastolic changes early after the Fontan operation are more likely secondary to unloading. Changes occurring over time are more likely related to changes in ventricular compliance. Progressive increase in ventricular stiffness and reduction in compliance might be one of the major mechanisms explaining Fontan failure with progressive age.

The pulmonary circulation limits cardiac output after the Fontan operation

A characteristic feature of the Fontan circuit is the lack of pulsatile pulmonary blood flow through the pulmonary vascular bed. In the normal biventricular circulation, PVR is generally not a limiting factor for determining cardiac output. In ischemic heart disease and cardiomyopathy, decreased cardiac pump function limits cardiac output. After the Fontan procedure the pulmonary circulation limits the preload reserve to the FSV and determines the cardiac output response [10,18]. This is comparable to obstructed inflow after Mustard repair, primary pulmonary hypertension, constrictive pericarditis, and mitral stenosis.

Different factors influence the amount of pulmonary blood flow and cardiac output after the Fontan operation. The first limiting factor is the energy loss in the surgical connections. The presence of unobstructed surgical connections between the caval veins and the PAs is a requirement for optimal Fontan circulation function. Any degree of obstruction within the Fontan connections will reduce cardiac output. The PAs need to be good-sized and unobstructed. PVR further determines pulmonary blood flow. Even a mild increase in PVR reduces pulmonary blood supply and cardiac output [19]. Pulmonary vasodilators like sildenafil positively influence cardiac output and exercise capacity in Fontan patients but to a limited extent [20–22]. Pulmonary venous obstruction is another important factor determining pulmonary blood flow. Some patients with FSV also have anomalous pulmonary venous connection that requires surgical intervention; they are at high risk for obstruction. The extracardiac Fontan conduit may also compress the adjacent right pulmonary veins. Further, the left lower pulmonary vein may become compressed between the heart, the descending aorta, and the spine.

In the Fontan circuit, pulmonary blood flow will increase with inspiration and decrease with expiration following respiratory variations in intrathoracic pressure [23]. Studying respiratory variation in Fontan patients has provided interesting physiologic information. Increased intrathoracic pressure due to airway obstruction or positive pressure ventilation reduces pulmonary blood flow and is detrimental for Fontan physiology [24]. Negative pressure ventilation is considered beneficial and results in increased cardiac output.

Fontan modifications

Since its original description, the Fontan circuit has undergone several surgical modifications (Figure 29.5) [25,26]. The original Fontan circuit in patients with tricuspid atresia included a valved homograft between the RA appendage and the right pulmonary artery in two patients and direct anastomosis without a conduit in one. The use of valved conduits in the Fontan circulation was found to be associated with a high degree of stenosis, and the direct atriopulmonary connection became the most commonly used modification in the 1980s. It was thought that including the right atrium in the Fontan connection would be beneficial for pulmonary hemodynamics due to the presence of the atrial "kick." However, elevated atrial pressure caused progressive right atrial dilation, reducing the energetic efficiency and becoming a substrate for atrial arrhythmia. Experimental and computational modeling was subsequently performed showing that a total cavopulmonary connection (TCPC) would be hemodynamically more favorable and would result in less energy and power loss in the conduit when compared to atriopulmonary connection [27,28]. In this circuit, the venae cavae are connected directly to the right pulmonary artery (RPA). The superior vena cava (SVC) is connected to the RPA (bidirectional Glenn

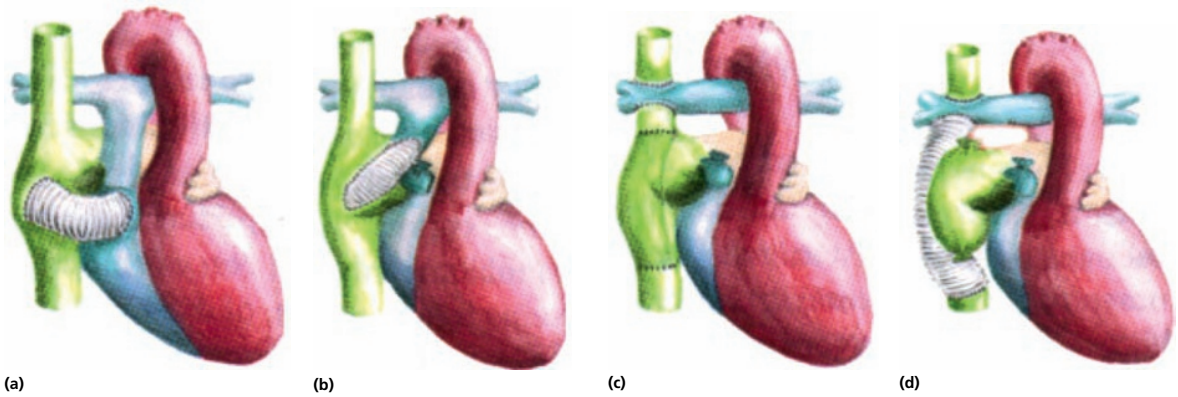

Figure 29.5 Different modifications of the Fontan operation. **(a)** Original Fontan operation with valve graft from right atrium to hypoplastic right ventricle connecting to the pulmonary artery. **(b)** Atriopulmonary connection. The right atrium is connected to the pulmonary artery. **(c)** Total cavopulmonary connection with intra-atrial tunnel. **(d)** Total cavopulmonary connection with extracardiac conduit.

shunt) and the inferior vena cava (IVC) is connected through an intra-atrial (lateral tunnel) baffle or by an extracardiac conduit. The benefits of the lateral tunnel Fontan include use in small children and potential for growth. The potential drawback is that there is substrate for atrial arrhythmia as a result of the suture line in the atrium and the exposure of atrial tissue to high pressure. To avoid these problems, the extracardiac conduit was introduced. This procedure consists of a tube graft between the inferior vena cava and the PA placed externally around the right atrium. This circuit leaves the entire atrium at low pressure, has minimal atrial suture lines, and can be performed without aortic cross-clamping. However, this tube graft has no growth potential and therefore is typically offered to larger patients (generally between 2 and 3 years of life). It remains to be determined whether the extracardiac conduit will decrease the arrhythmia risk and is hemodynamically favorable. When assessing a patient with a Fontan circulation, it is essential to know which type of connection has been made.

Current strategy towards a Fontan circulation

In the newborn period it is impossible to create a Fontan circulation because of the elevated PVR, which progressively decreases during the first weeks after birth. Even when PVR falls, a staged approach to Fontan completion is preferred, with the superior and inferior caval veins incorporated into the systemic venous chamber in two separate stages. Thus, the body adapts progressively to the new hemodynamic state and ventricular unloading is staged, reducing the operative morbidity and mortality. In the neonatal period, clinical management aims at achieving unrestricted flow to the aorta (when required: arch repair, Damus–Kaye–Stansel, Norwood procedure), appropriately limited flow to the lungs (when required: PA band, aortopulmonary shunt, stenting of the arterial duct), and unrestricted return of blood to the ventricle (if required: balloon septostomy, pulmonary venous connection). Between 4 and 8 months of age, the bidirectional Glenn shunt is performed. After the Glenn shunt, the patient remains mildly cyanotic because the desaturated blood from the IVC still connects to the systemic ventricle and the aorta. In infants the distribution of blood flow between the upper and lower body is around 2 : 2 which helps the efficiency of the bidirectional Glenn shunt in the first 2 years of life. As the lower body grows faster than the upper body this ratio changes and is reversed in adults with around twice as much blood coming from the IVC compared to the SVC. Typically, the Fontan circuit is completed between 2 and 5 years of age, incorporating the IVC into the Fontan circuit.

At the time of Fontan completion, often a small fenestration is created between the systemic venous pathway and the pulmonary venous atrium, either routinely or only in "high-risk" patients. The fenestration allows a residual right-to-left shunt, thereby reducing systemic venous pressure and increasing preload of the systemic ventricle at the expense of cyanosis. A fenestration has been shown to reduce operative mortality and morbidity (e.g., pleural drainage). It can be closed by a percutaneous intervention weeks or months after adaptation of the body to the new hemodynamic condition, particularly if marked cyanosis occurs with exercise.

Complications after the Fontan operation are common and relate to the increased systemic venous pressure and chronic low cardiac output. After surgery, there are clinically important early and late adverse outcomes, including mortality, exercise intolerance, ventricular dysfunction, rhythm and conduction abnormalities, hepatomegaly with secondary liver dysfunction, and potential for development of liver fibrosis or cirrhosis and adenocarcinoma, lymphatic dysfunction, protein-losing enteropathy, plastic bronchitis, thrombus formation, ascites, and peripheral edema.

Imaging

Before scanning a patient who has undergone a Fontan operation, it is essential to first review the underlying cardiac anatomy and previous surgical history. The ventricular morphology (see Chapter 28) needs to be known as this influences measurements and interpretation of functional information. It is essential to be aware of the type of Fontan connection as well as any additional cardiac procedures before starting to scan. This includes information on previous arch surgery, the presence of a Damus–Kaye–Stansel (DKS) connection, previous valve surgery, type of previous shunt if performed (modified Blalock–Taussig shunt or other), interventions on the pulmonary arteries (e.g., patch arterioplasty, balloon dilatation, stent implantation), and interventions on the pulmonary veins. Additionally, the echocardiographer should know the clinical indication for the scan and the patient's current clinical status, including absence or presence of symptoms and any specific clinical concerns. Some issues such as residual cyanosis, ascites, protein-losing enteropathy, or other signs of Fontan failure may require specific image acquisition as detailed later. Access to previously performed imaging studies greatly facilitates interpretation of findings and detection of changes. Comparison between studies should be easy and should be routine in the review process. To facilitate this comparison, digital storage of clips and usage of standard scanning protocols is highly recommended. As these patients have frequently undergone multiple surgeries, acoustic windows may be challenging, especially with increasing age.

Key elements

- Assessment of the Fontan pathway:
  - Presence of fenestration and transfenestration mean gradient
  - Presence of thrombus in Fontan pathway
  - Obstruction of Fontan connections
- Assessment of the pulmonary venous chamber:
  - Document unrestricted atrial communication
  - Assess for pulmonary venous obstruction
- Assessment of AV valve function:
  - AV valve regurgitation: severity grade and mechanism
  - AV valve stenosis: mean inflow gradient
- Assessment of single ventricular function:
  - Ventricular size measurements
  - Systolic performance
- Assessment of outflow tracts, semilunar valve(s), ascending aorta, and aortic arch:
  - Determine semilunar valve competency
  - Assess for outflow obstruction to aorta
  - Assess the DKS connection
  - Assess for residual or recurrent arch obstruction
- Assessment of branch pulmonary arteries:
  - Determine narrowing, stenosis, and competitive flow

Assessment of Fontan connections, pulmonary arteries, and pulmonary veins

Typically, it is recommended to begin the scan with subxiphoid imaging. Coronal or subxiphoid sagittal views in particular allow for visualization of the IVC and its connection to the Fontan baffle. Color flow imaging and pulsed-wave Doppler tracings in this view are used to assess for obstruction (Figure 29.6, Videos 29.1–29.6). The IVC and hepatic veins are typically dilated and spontaneous contrast is often noted. Flow velocities should be low (generally <20–30 cm/s). For pulsed-wave Doppler assessment, the sweep speed should be reduced in order to record flow throughout the respiratory cycle. Normally a low-velocity continuous systolic and diastolic flow pattern is detected (Figure 29.7). Usually, the flow increases with inspiration and decreases with expiration. The presence of respiratory variation suggests that intrathoracic pressure changes are well transmitted in the Fontan conduit, a sign that the Fontan connections are unobstructed. Absence of respiratory variation or the presence of reverse flow in the cardiac cycle is abnormal. Retrograde flow during systole may be seen in the setting of AV valve regurgitation or be due to the presence of significant competitive collateral flow. Flow reversal during diastole may be present in failing Fontan circulation or in the presence of atrial arrhythmia (increased pressure in the Fontan circuit). Lack of respiratory variation should raise suspicion of Fontan pathway obstruction. In the intra-atrial tunnel or an extracardiac conduit, the connection between the IVC may be well visualized using subxiphoid long- and short-axis sweeps. Subxiphoid, apical, and parasternal views are combined to assess the Fontan baffle (Figures 29.8–29.10). This assessment includes looking for tunnel dilation, presence of clots, and residual fenestration or baffle leaks (Videos 29.1–29.10). If a fenestration is present, a pulsed Doppler tracing of the fenestration flow should be acquired (Figure 29.11). An estimate of the pressure gradient between the systemic and pulmonary venous chambers can be determined by obtaining the mean gradient across the fenestration (transpulmonary gradient). If the fenestration has been closed with a device, the position of the device should be evaluated as well as the presence of a residual shunt.

The superior connection between the tunnel/conduit and the pulmonary arteries is often difficult to image. The apical, parasternal long-axis, and particularly the suprasternal views are helpful in visualizing this region (Videos 29.11–29.13). Typically, the atriopulmonary connection results in progressive, marked atrial dilation with low flow velocities, spontaneous contrast, and potential for thrombus formation. Other types of connections involving valved conduits should be carefully inspected for valve dysfunction (especially stenosis) and thrombus formation. Color flow using low Nyquist settings should be used to visualize the surgical anastomosis sites of the Fontan connections. In the case of obstruction, the flow pattern in the baffle becomes continuous throughout the respiratory cycle as the gradient can persist during expiration.

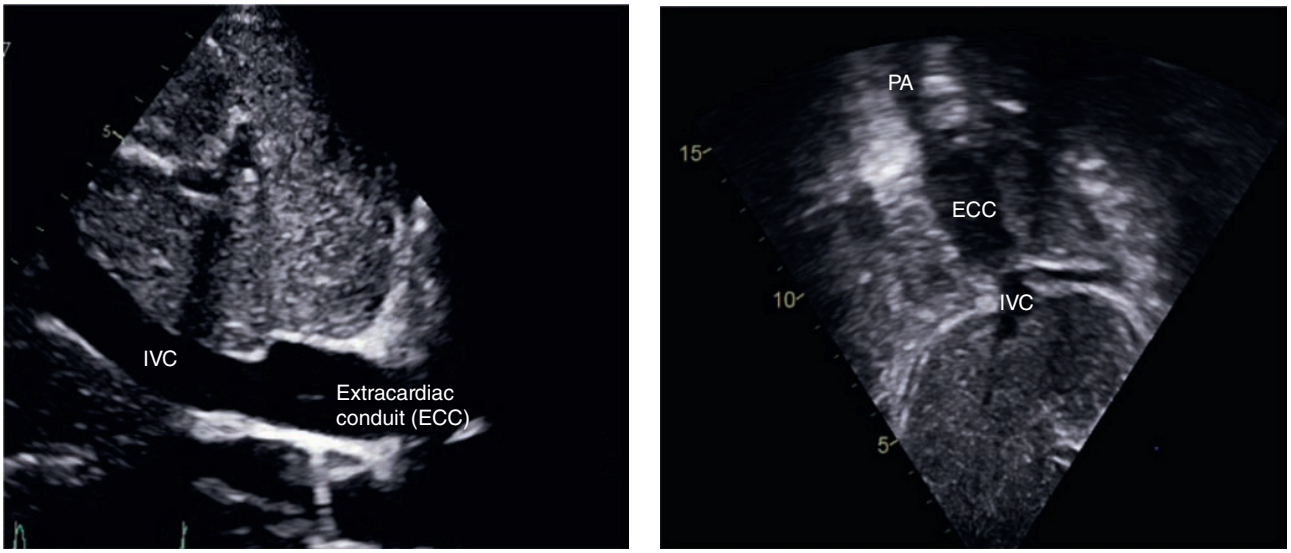

(a) (b)

Figure 29.6 The connection between the inferior vena cava (IVC) and the extracardiac conduit (ECC). **(a)** The connection between the IVC and the EEC is demonstrated from a subxiphoid long-axis view. The IVC is dilated. The IVC–ECC connection is widely patent as seen by 2D imaging. **(b)** Subxiphoid "bicaval" view demonstrating the extracardiac Fontan connection going up to the pulmonary artery (PA).

If transthoracic imaging is insufficient, transesophageal echocardiography (TEE) may provide better imaging of the conduit, tunnel, or atrium.

In patients with a lateral tunnel or extracardiac-type Fontan connection, it is imperative to evaluate the connection between the SVC and the RPA (Glenn anastomosis) (Figure 29.12, Video 29.11). This area is best visualized from the suprasternal frontal view. In this view, the flow into the branch pulmonary arteries may be imaged although adequate imaging is challenging in older patients. The flow pattern in the SVC resembles that in the IVC with increased flow with inspiration and decreased flow with expiration. If flow acceleration is noted at the anastomosis site, a pulsed Doppler tracing can be obtained and mean gradient calculated. Thrombus may be present in the SVC or the innominate vein, especially if a central line is present. In case of bilateral superior venae cavae, both anastomotic connections should be visualized. Generally, the left SVC is smaller than the right, and obstruction of the left-sided

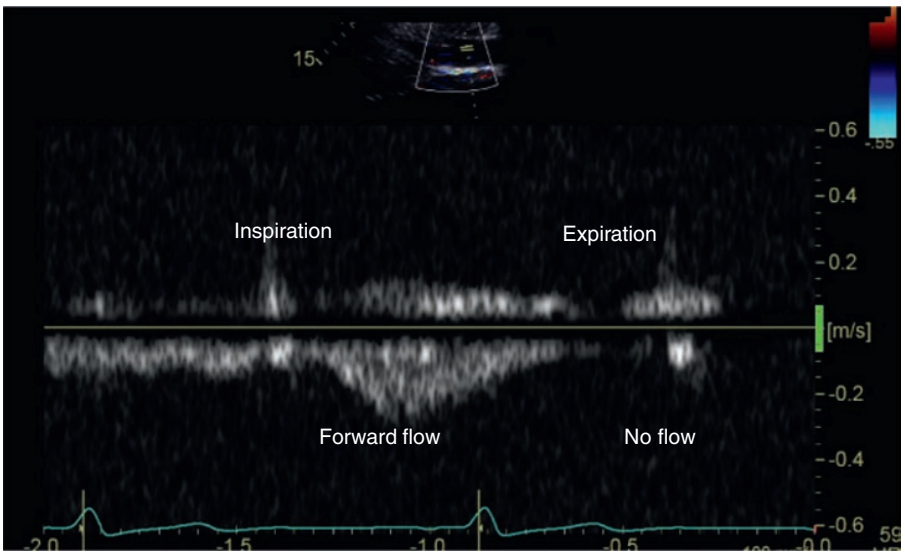

Figure 29.7 Flow in the hepatic vein–inferior vena cava (IVC) junction. The increase in flow during inspiration and almost absent flow during expiration can be demonstrated on the pulsed-wave Doppler tracing. The presence of respiratory variation in the hepatic and IVC flows suggests the presence of an unobstructed connection.

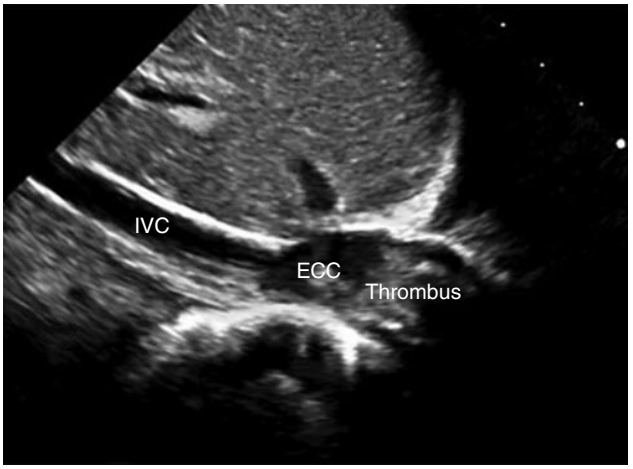

Figure 29.8 This image was obtained in a Fontan patient a few days after his Fontan completion. This subxiphoid long-axis view demonstrates the presence of a large thrombus in the extracardiac conduit (ECC). This was confirmed by urgent cardiac catheterization. IVC, inferior vena cava.

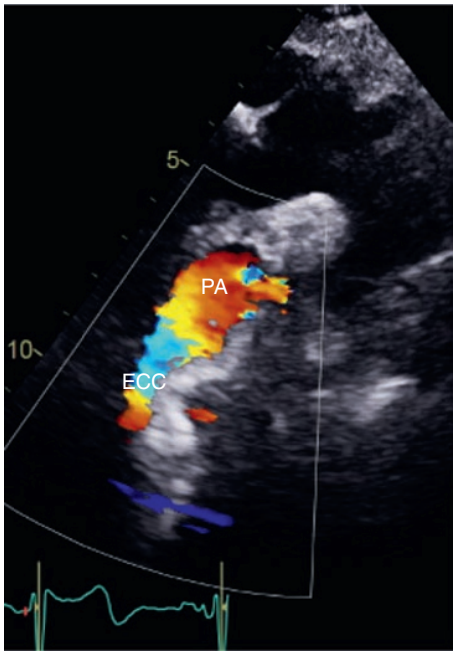

Figure 29.9 Suprasternal view to image the Fontan connection. In this suprasternal view the connection between the Fontan conduit (ECC) and the pulmonary artery (PA) can be demonstrated with the flow from the conduit unobstructed to the PA.

anastomosis is more common. However, the size and relative flow rates in the superior venae cavae vary. Also, it is worth noting that the PA segment between the right and left cavopulmonary anastomoses may become hypoplastic over time because it receives little flow.

The branch pulmonary arteries are also best visualized using suprasternal and high parasternal views (Figures 29.12 and 29.13, Videos 29.12 and 29.13). The proximal RPA is visualized from the suprasternal frontal view. When rotating the transducer into a sagittal (arch) view, the left pulmonary artery (LPA) may be seen coursing toward the left hilum. Pulsed Doppler tracings in both pulmonary arteries are recorded to evaluate the flow pattern. If stenosis is present, a continuous flow pattern with an elevated mean gradient is seen. If a PA stent is present, the metal frame often causes shadowing and reverberations, which can make it difficult to demonstrate flow. Color flow seen distal to the stent is reassuring. Flow reversal in the branch pulmonary arteries suggests increased PVR or the presence of competitive flow from significant aortopulmonary collaterals.

The pulmonary veins should also be interrogated after the Fontan procedure. Due to the position of the lateral tunnel and

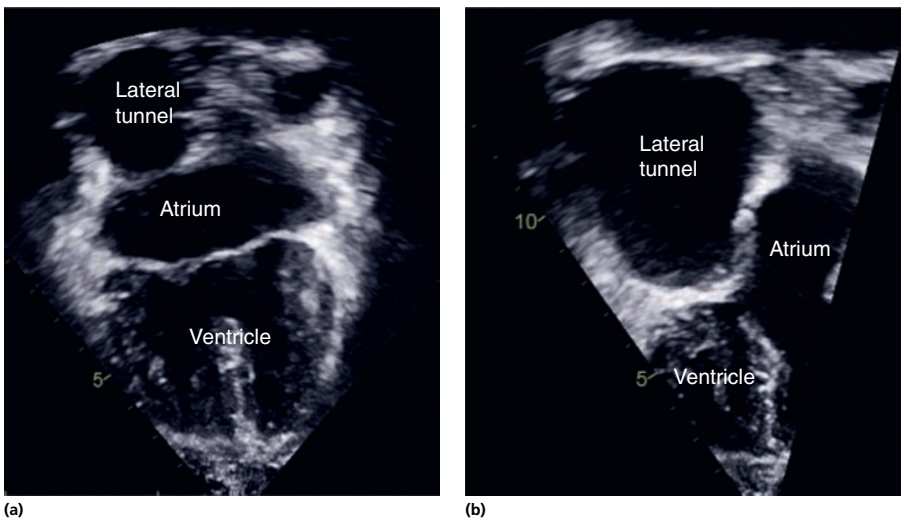

(a) (b)

Figure 29.10 Dilated lateral tunnel. This patient has an intra-atrial tunnel Fontan-type connection. The apical four- **(a)** and two-chamber **(b)** views demonstrate the dilated atrial tunnel.

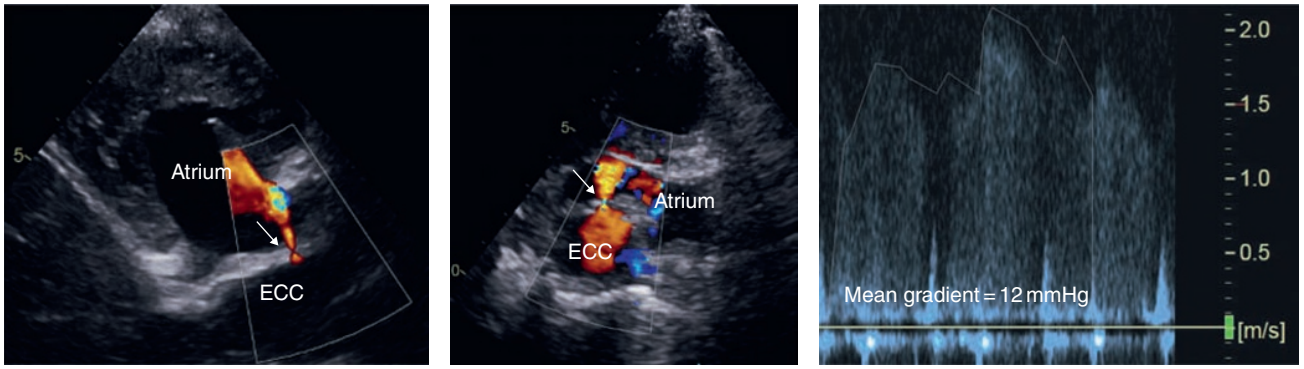

Figure 29.11 Fenestration in an extracardiac conduit (ECC). **(a)** The long-axis view of the conduit with the small fenestration as seen on color Doppler. **(b)** The fenestration in a short-axis cut through the conduit. The arrows point to the fenestration. **(c)** The spectral Doppler tracing measuring a mean gradient of 12 mmHg. This reflects the transpulmonary gradient (pressure difference between the Fontan and the atrium).

the extracardiac conduit close to the right upper and lower pulmonary veins, this can cause compression on the veins (Videos 29.14 and 29.15). Significant dilatation of the lateral tunnel or the right atrium may cause compression of the pulmonary veins (Figure 29.14, Video 29.16). Pulmonary venous obstruction in a Fontan circuit can be difficult to detect by echocardiography and may require additional imaging by cardiac CT, MRI, or cardiac catheterization.

Assessment of atrioventricular valve function

Careful evaluation of the AV valves is performed in every Fontan patient. Significant AV valve regurgitation is associated with morbidity and mortality in this patient population.

AV valve regurgitation is a common problem after the Fontan operation, particularly in the presence of a common AV valve or a dominant tricuspid valve. Echocardiographic assessment includes evaluation of the severity of AV valve regurgitation as

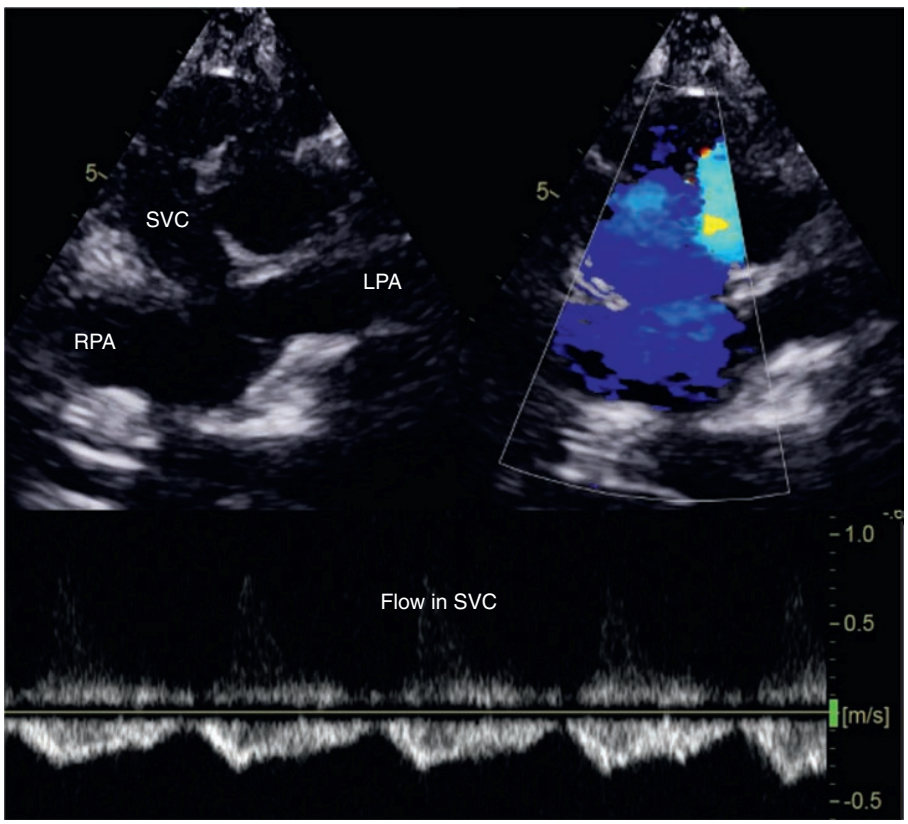

Figure 29.12 This suprasternal view demonstrates the connection between the superior vena cava (SVC) and the left and right pulmonary arteries (LPA and RPA). The flow is laminar into good-sized pulmonary arteries with low-velocity flow as shown on spectral Doppler.

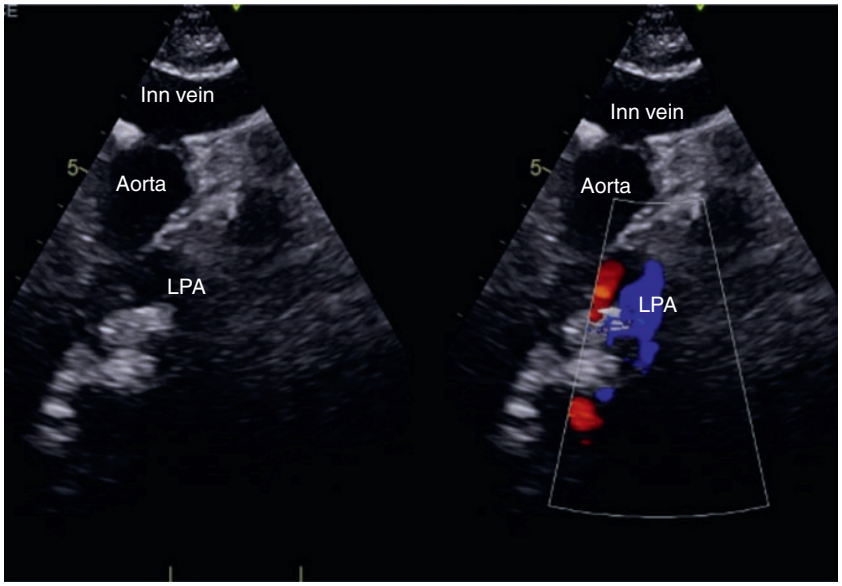

Figure 29.13 The suprasternal view is generally a good window to image the left pulmonary artery (LPA). On this view it is imaged below the aorta with laminar flow. In patients after aortic arch reconstruction, the LPA can be compressed by the enlarged aorta given their close spatial relationship. Inn vein, innominate vein.

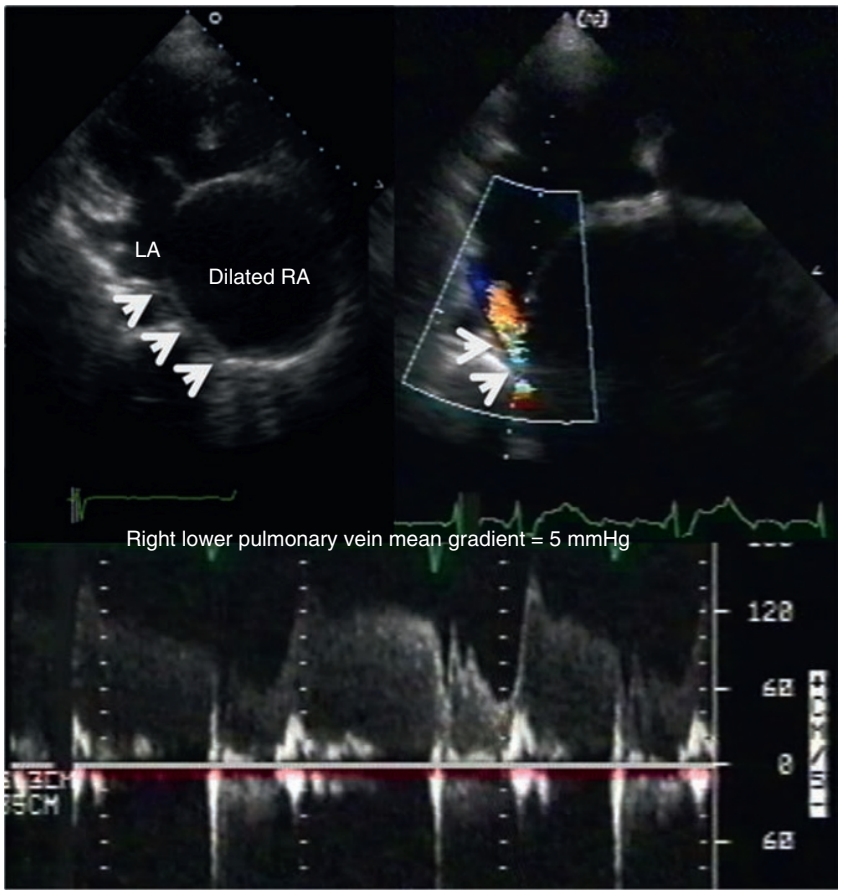

Figure 29.14 This patient has an atriopulmonary connection with important dilation of the right atrium (RA), causing compression on the right upper pulmonary vein (arrows) with turbulent flow in the pulmonary vein and a mean gradient of 4–5 mmHg. LA, left atrium. *Source*: Courtesy of Dr. F. Meijboom.

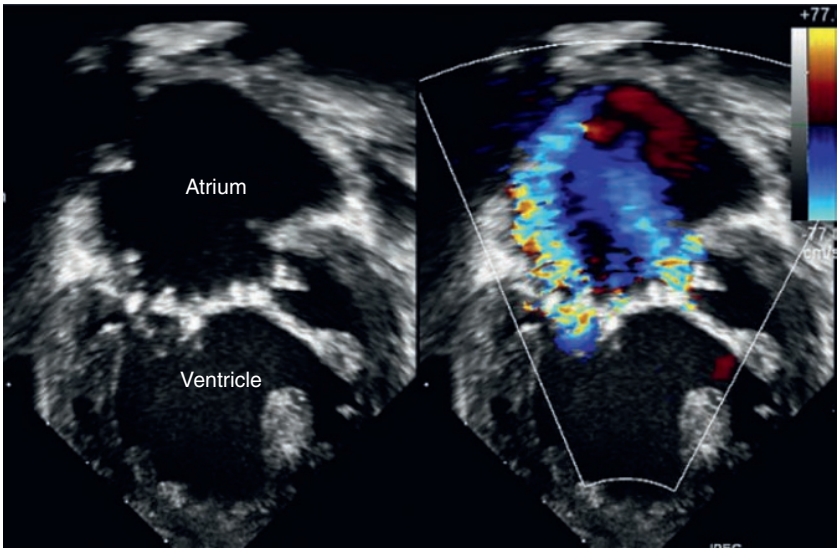

Figure 29.15 Common atrioventricular (AV) valve regurgitation in a patient with unbalanced AV septal defect after Fontan surgery. The color Doppler image obtained from the apical four-chamber view shows two jets of valve regurgitation resulting in both atrial and ventricular dilation.

well as identification of the mechanism (Figure 29.15, Videos 29.17 and 29.18). Assessment of the severity of regurgitation is largely based on qualitative assessment using color flow. Different imaging planes should be used for assessing the size of the regurgitant jet in three dimensions. The jet width at the level of the leaflets generally is a good indicator of the severity of the regurgitation. Jet width assessment becomes more challenging when multiple jets are present. A combination of jet width, jet area, and jet length into the atrium generally allows for subjective assessment as mild, moderate, or severe. If more than mild, identifying the mechanism of regurgitation becomes important. Common mechanisms for regurgitation are valve dysplasia (e.g., thickened leaflets), leaflet(s) prolapse, restricted leaflet motion due to abnormal tethering, papillary muscle splaying associated with ventricular dilation, and annular dilation [29]. Describing the mechanisms of regurgitation requires scanning the valve in multiple planes. Three-dimensional echocardiography may provide additional information on the AV valve in a FSV [30]. Further improvements in spatial and temporal resolutions of this technique as well as further refinement in imaging processing will allow better definition of leaflet abnormalities and a more detailed description of the subvalvar apparatus.

After valve repair, careful follow-up of the surgical result is required. In case of prosthetic valve insertion, evaluation of prosthetic valve function is essential (Figure 29.16, Video 29.18). Perivalvar leaks can be present and should be distinguished

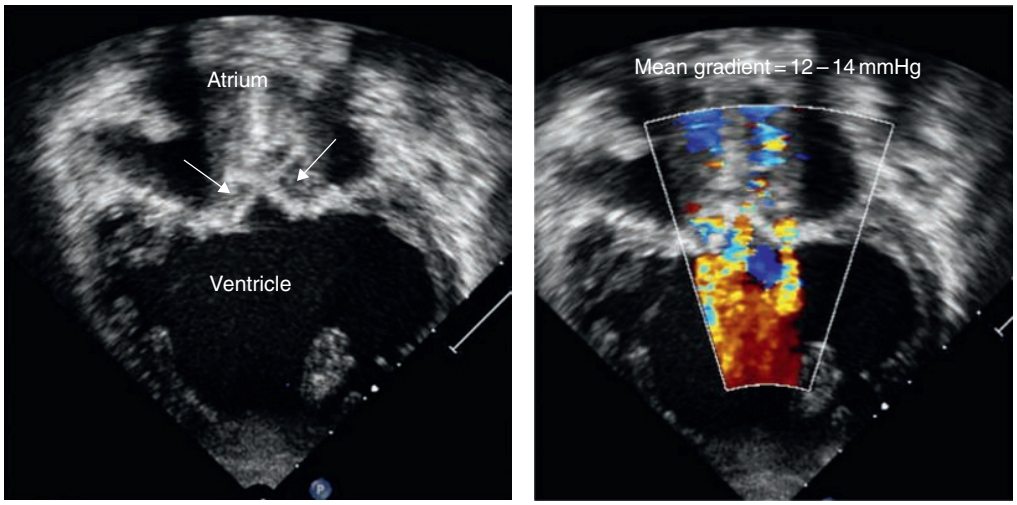

Figure 29.16 A Fontan patient with a prosthetic atrioventricular (AV) valve (the same patient as in Figure 29.15 after valve replacement). He underwent insertion of a metallic prosthetic AV valve that unfortunately quickly developed a significant inflow gradient, despite adequate anticoagulation levels. The mean gradient was measured between 12 and 14 mmHg. The arrows point to the leaflets of the prosthetic valve.

from regurgitation related to deficient prosthetic valve function. The low flow profile through the prosthetic valve makes it theoretically more prone to valve thrombosis. After valve repair, close monitoring of FSV function is paramount. The long-term outcome of patients undergoing AV valve repair in the context of FSV palliation is worse than that for case-matched patients not requiring valve surgery [31].

AV valve stenosis is rare but can be present after valve repair or prosthetic valve replacement. Inflow through the valve(s) is assessed using color flow and pulsed-wave Doppler from the apical views. When a gradient is present, continuous-wave Doppler should be obtained as aliasing may occur. The mean gradient should be calculated throughout the respiratory cycle and should be measured in at least three cardiac cycles. For prosthetic valves, a certain low mean gradient is common and known for the specific valve types. If significant regurgitation is present, the mean inflow gradient may be overestimated due to increased flow. Documentation of serial gradients is key for this purpose.

Assessment of outflow tracts, ascending aorta, and aortic arch

In FSV, the outflow tract from the dominant ventricle connects the ventricle to the aorta. Outflow tract obstruction, if present, causes chronic pressure loading with secondary concentric hypertrophy, which is detrimental for the long-term preservation of ventricular function. It can further limit the output from the single ventricle and will result in progressive ventricular hypertrophy that could be detrimental for diastolic function. Any type of outflow obstruction is thus detrimental for a Fontan patient and must be detected early. The mechanism causing outflow tract obstruction is most commonly subvalvar. As described in detail in Chapter 28, a typical example is double-inlet left ventricle with transposition of the great arteries where the ventricular septal defect (VSD) to the infundibular outlet chamber may become restrictive and thus cause subaortic obstruction. In patients at risk for this type of obstruction, typically a DKS procedure connecting both outflow tracts to the aorta is performed. Detailed imaging of the outflow tracts is an essential part of the echocardiographic examination in all Fontan patients, especially in those who did not undergo a DKS procedure to ensure unobstructed flow (Video 29.19). Different acoustic windows (subxiphoid, apical, and parasternal long-axis views) can be used to image the outflow tracts. Color Doppler, pulsed-wave, and continuous-wave Doppler traces are obtained with particular attention to optimal alignment of the ultrasound beam with the outflow tract. The peak and mean gradients should be measured. If a gradient is detected, the location of and the mechanism(s) causing the gradient should be defined. This can include subaortic obstruction due to a restrictive VSD, a membranous/fibrous ring, or valvar obstruction. The DKS connection between the ascending aorta and previous pulmonary trunk is imaged. Obstruction at the DKS anastomosis can compromise coronary artery blood flow resulting in ischemia and ventricular dysfunction. Semilunar valve function should also be evaluated. When the pulmonary valve is assigned to the aortic position (neoaorta), regurgitation is prevalent. A DKS connection can distort one or both semilunar valves and cause regurgitation. Fortunately, important semilunar valve regurgitation is unusual in FSV.

Assessment of the aortic/neoaortic root includes measurements of root size and shape. The ascending aorta is imaged from the parasternal and suprasternal views and the largest diameter is measured in systole. After extensive aortic reconstruction, progressive dilation of the aortic root and ascending aorta has been described, resulting in aneurysm formation that requires reintervention.

In patients who underwent aortic arch reconstruction or coarctation surgery, assessment for residual arch obstruction is essential. Residual arch obstruction and coarctation of the aorta cause arterial hypertension and a significant increase in afterload to the FSV. Even a mild gradient across the aortic arch can result in ventricular dysfunction and affect long-term diastolic dysfunction. The suprasternal window is best to image the arch. Color Doppler and continuous-wave Doppler are used to assess the peak gradient across the arch and the descending aorta. In a reconstructed arch, the proximal arch gradient should be incorporated into the Bernoulli equation to achieve the most accurate arch gradient. In adult patients, the aortic arch can be difficult to image. A good alternative for ruling out residual arch obstruction is obtaining a pulsed-wave Doppler tracing of the abdominal aorta from the subxiphoid views. The absence of significant diastolic anterograde flow in the abdominal aorta rules out significant residual arch obstruction.

Assessment of single ventricular function

One of the most challenging parts of the echocardiogram in patients after the Fontan procedure is the assessment of ventricular function. Application of standard methods of assessment of the normal LV to the FSV poses a significant challenge, mainly related to variability in morphology and loading conditions. Assessment of ventricular function requires assessment of both systolic and diastolic function.

Systolic performance

The most widespread technique used to assess systolic ventricular function in patients after the Fontan operation is *subjective assessment* or "eyeball technique." Most echocardiography laboratories report ventricular function to be normal, mildly, moderately, or severely reduced based on subjective evaluation without any quantification. In two studies the qualitative assessment of FSV function was compared with MRI measurements of ejection fraction [32,33]. The studies looked at the reliability (intra- and interobserver variabilities) as well as the accuracy (agreement between echocardiographic assessment and cardiac MRI quantification) of the

assessment. The reproducibility of qualitative assessment was found to be moderate for LV morphology but weak for RV morphology. Also, the agreement between qualitative assessment by echocardiography and quantitative assessment by cardiac MRI was weak. Both studies found that image quality and reader's experience influenced the results. Notably, the discrepancy was more pronounced in the mild-to-moderate range of FSV dysfunction. This is not surprising as most readers are able to diagnose patients at both extremes of the spectrum with either severely reduced function or a completely normal ejection fraction. However, these observations highlight the importance of a quantitative approach to functional assessment of the FSV.

Quantitative approaches have been proposed and evaluated. A multicenter cohort study of the Fontan population used a *modified biplane Simpson method* to quantify FSV volumes and ejection fraction [33]. The reproducibility of this method was found to be good between the core echocardiography laboratory readers evaluating the studies, with better agreement for the LV than for the RV measurements. The agreement between echocardiographic and MRI quantitative assessments was weak, however, with systematic underestimation of FSV volumes by echocardiography. This is probably related to the different geometry of FSV when applying the Simpson formula or area–length method. Each laboratory should determine a standard approach for quantifying LV and RV systolic performance allowing for quantitative serial follow-up in the same patient. For a single LV, the biplane Simpson approach could be used in most cases. For a single RV, ejection fraction calculation based on standard formulas is not generally used in clinical practice. A good alternative is the calculation of *fractional area change* from an apical four-chamber view. This method correlates well with RV ejection fraction but requires good-quality images, which may be challenging in adults (Figure 29.17). Recently, *3D echocardiography* has been proposed as a good alternative technique for evaluating FSV volumes and ejection fraction. The method of summation of disks shows good reproducibility and accuracy [34]. However, it has recently been replaced by semi-automated (for the RV) or automated border detection and volumetric analysis. However, these analytical packages have been validated in biventricular hearts but not in FSV [12]. A major challenge with 3D echocardiography is that it can be very difficult to acquire a full volume of the entire FSV at reasonable frame rates; moreover, the anterior wall segments can be extremely difficult to visualize due to their anterior position in the chest just behind the sternum. This challenge increases in older children and in adult patients with a larger body size and more restricted acoustic windows.

Since volumetric data are difficult to obtain in FSV, alternative nongeometric methods have been proposed. Using blood pool Doppler signals, d*P*/d*t* can be calculated. This preload-sensitive method is based on a valve regurgitation jet or by using a modified method based on measurement of the isovolumetric contraction time (IVCT) and aortic diastolic blood pressure and assuming FSV end-diastolic pressure of 5 mmHg [35]. The regurgitation method requires the presence of at least a mild-to-moderate amount of regurgitation in order to be able to acquire a reliable Doppler signal, which is not possible in every patient. The method based on IVCT requires measuring time intervals on the inflow tracing and the outflow tracing, which requires that there is no change in heart rate between the two traces. An additional problem with this method is that the assumption about the end-diastolic pressure may be inaccurate. The reproducibility of d*P*/d*t* measurements was reported as being high but the value of d*P*/d*t* correlates only weakly with MRI-based measurement of

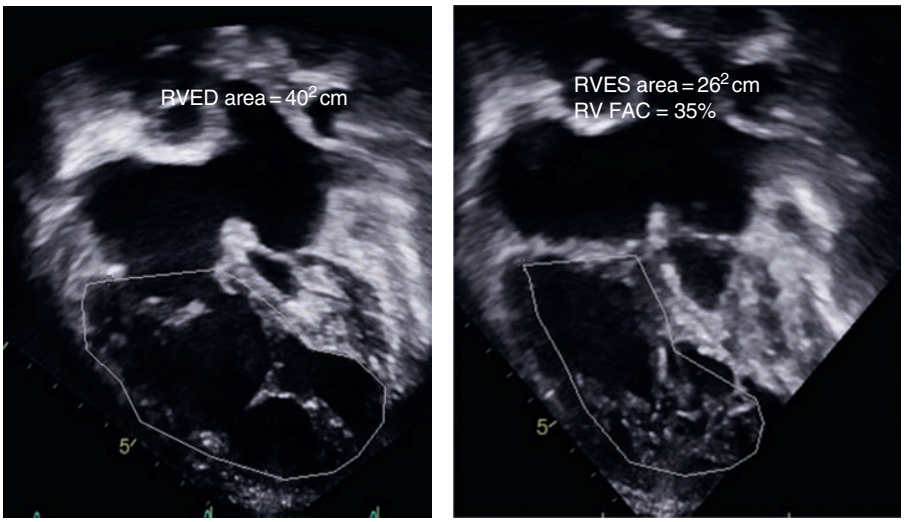

Figure 29.17 Quantification of single ventricular function. From an apical four-chamber view, fractional area change (FAC) can be measured by tracing the end-diastolic (RVED) and end-systolic (RVES) area and calculating the FAC, which in this patient was 35%.

ejection fraction [35]. An alternative nongeometric Doppler-based method is the *myocardial performance index* (MPI) or Tei index. This combined systolic–diastolic index of ventricular performance is calculated as:

$$\text{MPI} = \left(\text{IVRT} + \text{IVCT}\right) / \text{ET}$$

where IVRT is isovolumetric relaxation time and ET is ejection fraction. The index can be measured based on blood pool data (inflow and outflow) or tissue Doppler tracings. Tissue Doppler has the advantage that the measurement can be performed on the same cardiac cycle [35,36]. The reproducibility of this method has been moderate. In Fontan patients, MPI has been reported to be prolonged but the degree of prolongation does not correlate with ejection fraction as measured by MRI. MPI is preload and afterload sensitive and this may affect its clinical utility [37]. A potentially more attractive concept is the *ratio of systolic-to-diastolic duration* (S/D ratio) [38]. This measurement requires an AV valve regurgitation jet and measuring the duration of the regurgitation jet as the systolic duration and the inflow duration as the diastolic duration (Figure 29.18). When ventricular dysfunction develops, systolic duration prolongs, shortening diastolic inflow duration. In severe dysfunction, the heart spends most of the time in systole with only a short time in diastole, limiting diastolic filling. In normal children, the S/D ratio varies between 0.4 and 1.6 and is largely determined by heart rate [39]. In patients with hypoplastic left heart syndrome the S/D ratio has been shown to be elevated and higher in patients with RV dysfunction compared to patients with normal RV function [38]. However, when corrected for heart rate, the values were shown to be in the normal range [36]. More recent data in adult Fontan patients indicate that the S/D ratio relates to clinical outcomes and to filling pressures obtained by cardiac catheterization [40,41]. The use of nongeometric Doppler-derived timing parameters requires further investigation and currently is not part of routine clinical scans.

Tissue Doppler velocities can also be used in Fontan patients. Pulsed-wave tissue Doppler traces are relatively easy to obtain and are generally highly reproducible. For systolic function assessment, S′ velocity obtained in the lateral AV valve annuli is obtained and the peak systolic velocity (S′) is measured. As for other methods, S′ velocity is dependent on ventricular size, preload, and afterload and is also influenced by AV valve regurgitation. In the Fontan population, no correlation has been found between S′ velocity and ejection fraction as measured by cardiac MRI [35]. S′ is a local parameter of myocardial function reflecting longitudinal contraction in the basal part of the ventricle. Thus, regional myocardial dysfunction may be present in other areas, which can contribute to the lack of correlation. In serial follow-up studies, a reduction in S′ suggests a reduction in ventricular longitudinal function, which may warrant further investigation. The load dependency of tissue Doppler velocities may be overcome by measuring the acceleration of the tissue Doppler spike present during the isovolumic contraction period (isovolumic acceleration (IVA)). During this period, active force is developed in the myofibers resulting in a shape change in the ventricle just prior to ejection. IVA appears to be a relatively

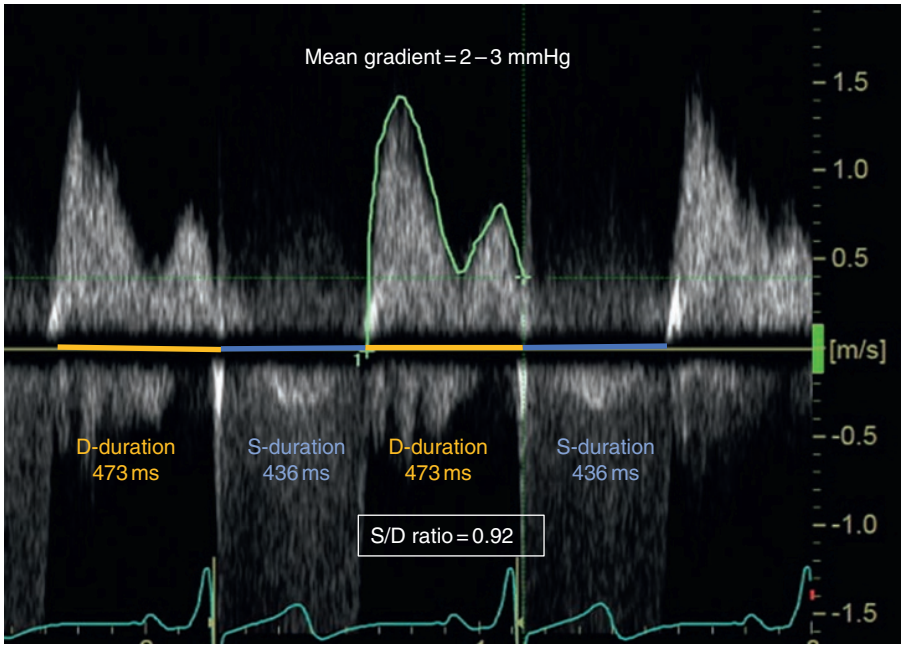

Figure 29.18 Assessment of S/D ratio. A continuous-wave Doppler tracing is obtained through the tricuspid valve inflow capturing the regurgitant jet. Systolic duration is measured from the duration of the tricuspid jet (blue color line). Diastolic duration is measured from the tricuspid inflow (yellow color line). The S/D ratio is calculated and was found to be normal in this patient. With progressive dysfunction, typically systolic duration increases and diastolic duration decreases, resulting in an increased S/D ratio.

load-independent measurement of cardiac contractility. It is however highly heart rate dependent and difficult to measure.

Most recently, the introduction of speckle-tracking technology has allowed the calculation of myocardial deformation or strain imaging in Fontan patients (Videos 29.20 and 29.21) [42]. This method was validated against myocardial strain measurements as obtained by MRI-based myocardial tagging [43]. Similar to other methods of functional assessment, strain measurements depend on loading conditions. Increased preload will increase myocardial deformation; increased afterload will result in decreased myocardial deformation. Presently, there is limited information on the clinical use of strain imaging in the Fontan population and its implementation in clinical practice. For the single LV, global longitudinal strain measurements can be obtained from the apical views while, for the single RV, the apical four-chamber view can be used (Figure 29.19). Typically for single LV, longitudinal strain values are within normal range, albeit often in the lower normal range [44]. For the RV, a single apical view can be used and traced. Values for RV strain are typically slightly lower than those for LV strain. Some groups have suggested adding short-axis circumferential strain to the evaluation of the single RV given that it appears to have more circumferential shortening compared to the normal RV. However, this methodology is difficult to standardize and has not been widely applied in clinical practice. The advantage of strain imaging is that is a highly reproducible method that can be applied in the serial follow-up of patients, allowing for a quantitative serial monitoring of cardiac function [45,46]. An additional application is that strain can be used to detect mechanical dyssynchrony as a potential mechanism that contributes to development of ventricular dysfunction. Dyssynchrony has been demonstrated to be present in about 10% of adult Fontan patients [47]. The presence of the classic dyssynchrony pattern can be easily recognized with early activation in one area, contralateral stretching, and late contraction in the opposing segments. Patients with classic pattern dyssynchrony, wide QRS duration, and ventricular dysfunction may benefit from resynchronization therapy (Videos 29.20 and 29.21) [48,49].

Diastolic performance

The development of diastolic dysfunction is probably one of the most important ventricular problems after Fontan palliation. Diastolic dysfunction has been shown to be highly prevalent with 72% of Fontan patients having diastolic abnormalities in a large cohort study [9]. The study proposed a grading system for

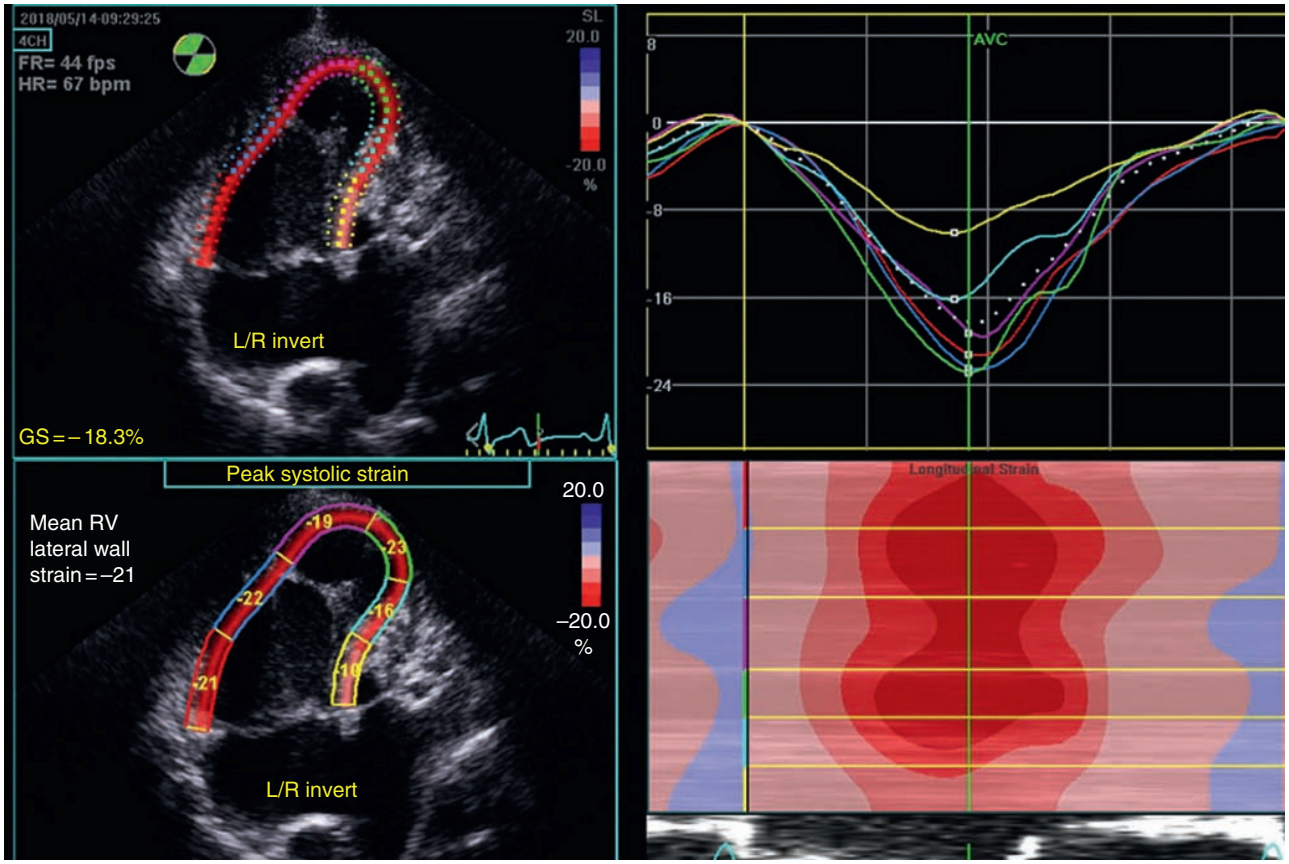

Figure 29.19 Strain measurements in the single right ventricle using speckle-tracking echocardiography. From an apical four-chamber view, longitudinal strain can be estimated. The mean RV lateral wall strain values are around –21%, within normal range for a systemic RV.

diastolic dysfunction with normal diastolic function defined as the ratio between the peak Doppler velocities of the early and atrial phases of AV valve inflow (E/A ratio) between 1 and 2, deceleration time (DT) of the AV valve inflow E wave ≥140 ms, and E/E′ ≤10. Impaired relaxation was defined as E/A ratio <1. Pseudo-normalization was identified when the E/A ratio was between 1 and 2 but DT <140 ms or E/E′>10 or flow propagation (FP) by color Doppler M-mode <55 cm/s. Restrictive physiology was based on E/A ratio >2. Importantly, this grading system was extrapolated from adult data and has not been validated against invasive pressure data in pediatric or adult Fontan patients. No associations were found between this classification and clinical parameters, suggesting this approach may not be of clinical value. Invasive studies trying to correlate diastolic measurements with invasive pressure measurements could not demonstrate clinically useful associations. It worth noting that most if not all echocardiographic parameters of diastolic function such as AV valve inflow, pulmonary venous flow, and tissue Doppler are influenced by heart rate, loading conditions, AV valve size and function, and FSV systolic function (Figure 29.20).

In the aging Fontan population, progressive decrease in ventricular compliance and increased end-diastolic pressure are often observed [46]. This is difficult to detect using noninvasive methods. In the adult population with a biventricular circulation E/E′ has been proposed as a useful parameter for identifying patients with increased filling pressures. In patients with FSV, the

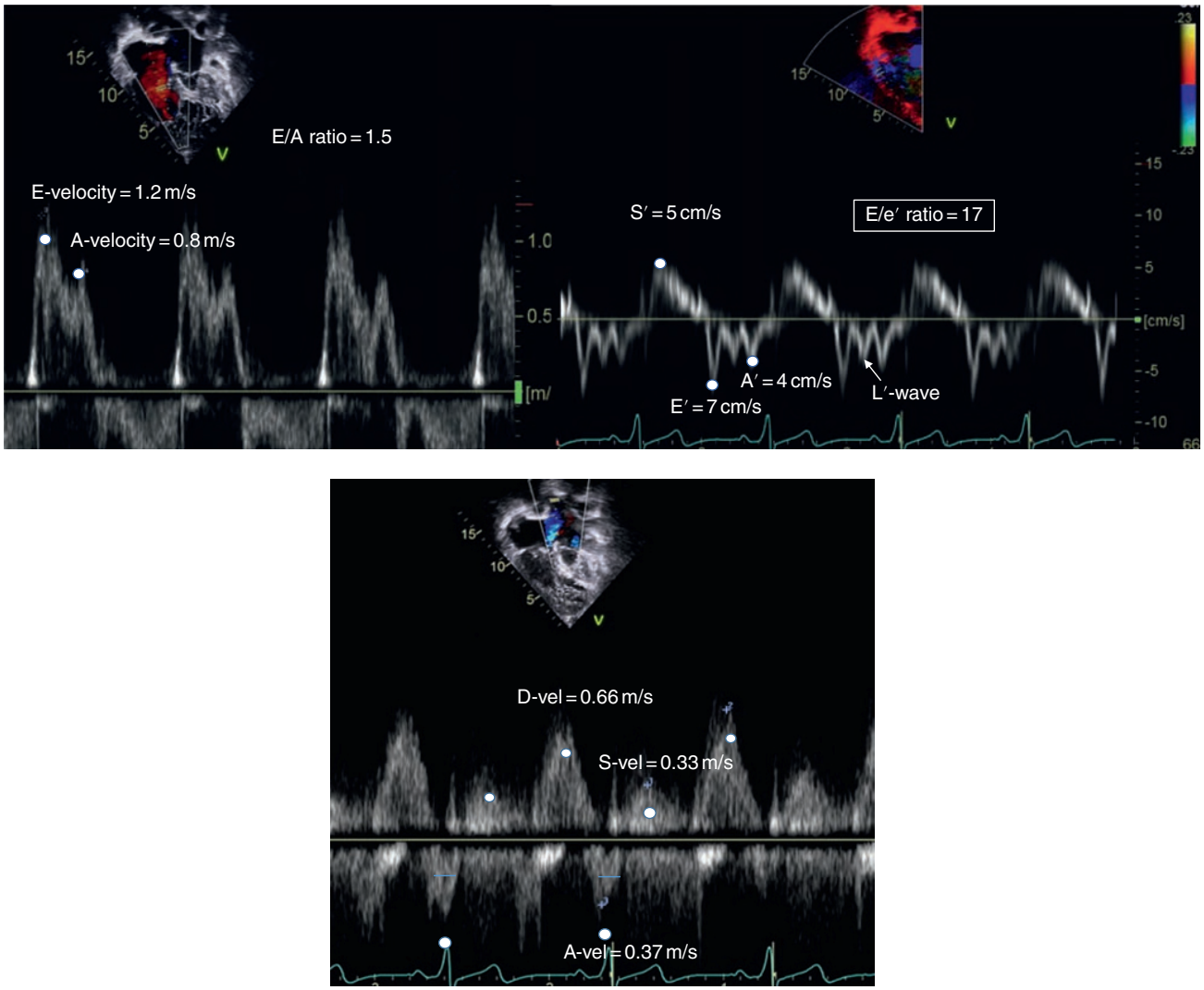

Figure 29.20 Diastolic function assessment in a patient with hypoplastic left heart syndrome after Fontan. The tricuspid inflow has increased E-velocity and high A-velocity with normal E/A ratio. The tissue Doppler tracing demonstrates low tissue Doppler velocities in the lateral tricuspid annulus. This is a common finding in postoperative patients. E′-velocity is higher than A′-velocity with mid-diastolic wave (L′-wave). This possibly suggests some delay in right ventricle (RV) relaxation with mid-diastolic motion. The E/E′ ratio is high but is not very useful in postoperative patients as E′-velocities are often reduced, possibly because of tethering of the RV base related to adhesions. The pulmonary vein tracing demonstrates high diastolic flow and somewhat reduced systolic flow with prominent A-wave reversals. This demonstrates that interpretation of the conventional diastolic parameters is extremely difficult in Fontan patients. The normal S/D ratio in this patient suggested normal filling pressure.

use of the E/E′ ratio is problematic because E velocity is influenced by AV valve size and E′ velocity is often preserved. Although diastolic dysfunction can be a primary cause of Fontan failure, current echocardiography techniques are not able to identify these patients based on currently established criteria. The diagnosis can even be challenging in the catheterization laboratory as filling pressures are highly dependent upon intravascular fluid status. Identification of FSV patients with reduced compliance is one of the remaining challenges in congenital cardiology. It is hoped that methods will soon be developed to provide information on tissue characteristics such as MRI-based T1 mapping for assessment of diffuse fibrosis or myocardial stiffness measurements based on ultrafast ultrasound.

Conclusion

Echocardiographic imaging in patients after the Fontan operation remains a significant challenge. It requires comprehensive understanding of the underlying complex morphology, the surgical techniques, and the unique physiology of the Fontan circulation. Although echocardiography is the standard routine follow-up technique, patients with Fontan failure or suspected complications will likely require additional imaging by MRI, CT, or angiography.

Videos

To access the video clips for this chapter, please go to wiley.com/go/lai-echo3.

Video 29.1 Connection between the inferior vena cava (IVC) and the extracardiac conduit. The connection between the IVC and the conduit is nicely demonstrated from a subxiphoid view by 2D imaging.

Video 29.2 Subxiphoid transhepatic view of an extracardiac conduit. In this view the conduit can be seen from inferior vena cava to the pulmonary artery.

Video 29.3 Lateral tunnel Fontan as seen from a subxiphoid view in 2D and color. The lateral tunnel is dilated. There is laminar flow with some flow acceleration on the tunnel to pulmonary artery connection.

Video 29.4 Lateral tunnel Fontan to pulmonary artery (PA) connection. This is a suprasternal view of the connection between the lateral tunnel and the PA. The flow going upwards (red) into the PA can be seen.

Video 29.5 Large thrombus in an extracardiac conduit. This was detected a few days after the Fontan operation. Notice the large clot in the conduit. There is spontaneous contrast in the inferior vena cava.

Video 29.6 Clot in a patient with a right atrium-to-pulmonary artery connection. This view shows the very large right atrium (RA) with spontaneous contrast and a large clot attached to the RA wall.

Video 29.7 Fenestration in an extracardiac conduit as seen from a long-axis view. Notice the small fenestration between the extracardiac conduit and the atrium.

Video 29.8 Fenestration in an extracardiac conduit as seen from a short-axis view. Notice the small fenestration between the extracardiac conduit and the atrium. This view provides the best alignment to obtain pulsed Doppler.

Video 29.9 Apical view of an extracardiac conduit. From an apical four-chamber view the conduit is typically seen in short axis located superior to the right-sided atrium.

Video 29.10 Apical long-axis view of an extracardiac conduit. From the apical four-chamber view the probe can be rotated by 90° clockwise and moved slightly rightward. This will show the conduit in long axis.

Video 29.11 Bidirectional Glenn connection. In this suprasternal view the superior vena cava-to-right pulmonary artery connection is shown. The proximal left pulmonary artery is seen as well.

Video 29.12 Focused view of the right pulmonary artery. In this suprasternal view the more distal right pulmonary artery can be seen.

Video 29.13 Focused view of the left pulmonary artery (LPA). In this suprasternal view the LPA can be seen in a patient after aortic arch reconstruction. The dilated aortic arch can be seen in short axis superior to the LPA.

Video 29.14 Apical four-chamber view demonstrating a dilated lateral tunnel. The image demonstrates the enlarged lateral tunnel. There is a device closing the fenestration, and a common atrioventricular valve.

Video 29.15 Modified apical view to better demonstrate lateral tunnel enlargement. The transducer is rotated towards a two-chamber view that shows the lateral tunnel enlargement better.

Video 29.16 Dilated right atrium in a patient with an atriopulmonary connection causing compression on the right lower pulmonary vein. In this view the very dilated right atrium can be seen with compression on the right lower pulmonary vein.

Video 29.17 Atrioventricular (AV) valve regurgitation in a patient with unbalanced AV septal defect. This patient underwent valvuloplasty during the Fontan surgery but still has severe regurgitation. The ventricle is severely dilated and moderately dysfunctional.

Video 29.18 Prosthetic valve in a Fontan patient. This patient underwent valve replacement with a metallic prosthetic valve. The echo demonstrated good prosthetic valve function.

Video 29.19 Damus–Kaye–Stansel anastomosis in a patient with double-inlet left ventricle with malposed great arteries. In this view a wide open anastomosis is demonstrated between the native aorta and the original pulmonary outflow. They join together to form the ascending aorta.

Video 29.20 Dyssynchrony in a patient with a single ventricle. Speckle tracking was used to quantify longitudinal deformation. From the images and curves it can be observed that the left lateral

wall is being stretched at the time the right lateral wall contracts. This causes significant dysfunction of the single ventricle with the patient developing symptoms of heart failure.

Video 29.21 Myssynchrony in a patient with a single ventricle. Resynchronization therapy resulted in significant improvement in global ventricular function and reverse remodeling.

Video 29.22 Y-graft Fontan connection. A Y-graft Fontan connection can be seen with the conduit splitting into a right and left pulmonary artery limb.

Video 29.23 Y-graft Fontan connection seen with color Doppler. LPA, left pulmonary artery.

References

1 Fontan F, Baudet E. Surgical repair of tricuspid atresia. *Thorax* 1971;**26**:240–8.
2 Gewillig M. The Fontan circulation. *Heart* 2005;**91**:839–46.
3 Gewillig M, Brown SC, van de Bruaene A, Rychik J. Providing a framework of principles for conceptualising the Fontan circulation. *Acta Paediatr* 2020;**109**:651–8.
4 Gewillig M, Brown SC. The Fontan circulation after 45 years: update in physiology. *Heart* 2016;**102**:1081–6.
5 Brooks PA, Khoo NS, Mackie AS, Hornberger LK. Right ventricular function in fetal hypoplastic left heart syndrome. *J Am Soc Echocardiogr* 2012;**25**:1068–74.
6 Bellsham-Revell HR, Tibby SM, Bell AJ, et al. Serial magnetic resonance imaging in hypoplastic left heart syndrome gives valuable insight into ventricular and vascular adaptation. *J Am Coll Cardiol* 2013;**61**:561–70.
7 Grosse-Wortmann L, Al-Otay A, Yoo SJ. Aortopulmonary collaterals after bidirectional cavopulmonary connection or Fontan completion: quantification with MRI. *Circ Cardiovasc Imaging* 2009;**2**:219–25.
8 Odenwald T, Quail MA, Giardini A, et al. Systemic to pulmonary collateral blood flow influences early outcomes following the total cavopulmonary connection. *Heart* 2012;**98**:934–40.
9 Anderson PA, Sleeper LA, Mahony L, et al. Contemporary outcomes after the Fontan procedure: a Pediatric Heart Network multicenter study. *J Am Coll Cardiol* 2008;**52**:85–98.
10 Senzaki H, Masutani S, Ishido H, et al. Cardiac rest and reserve function in patients with Fontan circulation. *J Am Coll Cardiol* 2006;**47**:2528.
11 Senzaki H, Masutani S, Kobayashi J, et al. Ventricular afterload and ventricular work in fontan circulation: comparison with normal two-ventricle circulation and single-ventricle circulation with blalock-taussig shunts. *Circulation* 2002;**105**:2885–92.
12 Kutty S, Graney BA, Khoo NS, et al. Serial assessment of right ventricular volume and function in surgically palliated hypoplastic left heart syndrome using real-time transthoracic three-dimensional echocardiography. *J Am Soc Echocardiogr* 2012;**25**:682–9.
13 Khairy P, Fernandes SM, Mayer JE, Jr., et al. Long-term survival, modes of death, and predictors of mortality in patients with Fontan surgery. *Circulation* 2008;**117**:85–92.
14 Gewillig M, Daenen W, Aubert A, Van der Hauwaert L. Abolishment of chronic volume overload. Implications for diastolic function of the systemic ventricle immediately after Fontan repair. *Circulation* 1992;**86**(5 Suppl):II93–9.
15 Penny DJ, Redington AN. Diastolic ventricular function after the Fontan operation. *Am J Cardiol* 1992;**69**:974–5.
16 Penny DJ, Rigby ML, Redington AN. Abnormal patterns of intraventricular flow and diastolic filling after the Fontan operation: evidence for incoordinate ventricular wall motion. *Br Heart J* 1991;**66**:375–8.
17 Redington A, Penny D. Regional ventricular wall motion abnormalities in tricuspid atresia after the Fontan procedure: flawed methodology may lead to a spurious finding of hypokinesia. *J Am Coll Cardiol* 1994;**24**:271.
18 Schmitt B, Steendijk P, Ovroutski S, et al. Pulmonary vascular resistance, collateral flow, and ventricular function in patients with a Fontan circulation at rest and during dobutamine stress. *Circ Cardiovasc Imaging* 2010;**3**:623–31.
19 Khambadkone S, Li J, de Leval MR, Cullen S, Deanfield JE, Redington AN. Basal pulmonary vascular resistance and nitric oxide responsiveness late after Fontan-type operation. *Circulation* 2003;**107**:3204–8.
20 Giardini A, Balducci A, Specchia S, Gargiulo G, Bonvicini M, Picchio FM. Effect of sildenafil on haemodynamic response to exercise and exercise capacity in Fontan patients. *Eur Heart J* 2008;**29**:1681–7.
21 Goldberg DJ, French B, Szwast AL, et al. Impact of sildenafil on echocardiographic indices of myocardial performance after the Fontan operation. *Pediatr Cardiol* 2012;**33**:689–96.
22 Goldberg DJ, Zak V, Goldstein BH, et al. Results of the FUEL Trial. *Circulation* 2020;**141**:641–51.
23 Penny DJ, Redington AN. Doppler echocardiographic evaluation of pulmonary blood flow after the Fontan operation: the role of the lungs. *Br Heart J* 1991;**66**:372–4.
24 Hsia TY, Khambadkone S, Redington AN, Migliavacca F, Deanfield JE, de Leval MR. Effects of respiration and gravity on infradiaphragmatic venous flow in normal and Fontan patients. *Circulation* 2000;**102**(19 Suppl 3):III148–53.
25 de Leval MR, Deanfield JE. Four decades of Fontan palliation. *Nat Rev Cardiol* 2010;**7**:520–7.
26 de Leval MR. Evolution of the Fontan-Kreutzer procedure. *Semin Thorac Cardiovasc Surg Pediatr Card Surg Annu* 2010;**13**:91–5.
27 de Leval MR, Kilner P, Gewillig M, Bull C. Total cavopulmonary connection: a logical alternative to atriopulmonary connection for complex Fontan operations. Experimental studies and early clinical experience. *J Thorac Cardiovasc Surg* 1988;**96**:682–95.
28 Van Haesdonck JM, Mertens L, Sizaire R, et al. Comparison by computerized numeric modeling of energy losses in different Fontan connections. *Circulation* 1995;**92**(9 Suppl):II322–6.
29 Bharucha T, Honjo O, Seller N, et al. Mechanisms of tricuspid valve regurgitation in hypoplastic left heart syndrome: a case-matched echocardiographic-surgical comparison study. *Eur Heart J Cardiovasc Imaging* 2013;**14**:135–41.
30 Takahashi K, Inage A, Rebeyka IM, et al. Real-time 3-dimensional echocardiography provides new insight into mechanisms of tricuspid valve regurgitation in patients with hypoplastic left heart syndrome. *Circulation* 2009;**120**:1091–8.
31 Honjo O, Atlin CR, Mertens L, et al. Atrioventricular valve repair in patients with functional single-ventricle physiology: impact of ventricular and valve function and morphology

on survival and reintervention. *J Thorac Cardiovasc Surg* 2011;**142**:326–35 e2.
32 Bellsham-Revell HR, Simpson JM, Miller OI, Bell AJ. Subjective evaluation of right ventricular systolic function in hypoplastic left heart syndrome: how accurate is it? *J Am Soc Echocardiogr* 2013;**26**:52–6.
33 Margossian R, Schwartz ML, Prakash A, et al. Comparison of echocardiographic and cardiac magnetic resonance imaging measurements of functional single ventricular volumes, mass, and ejection fraction (from the Pediatric Heart Network Fontan Cross-Sectional Study). *Am J Cardiol* 2009;**104**:419–28.
34 Soriano BD, Hoch M, Ithuralde A, et al. Matrix-array 3-dimensional echocardiographic assessment of volumes, mass, and ejection fraction in young pediatric patients with a functional single ventricle: a comparison study with cardiac magnetic resonance. *Circulation* 2008;**117**:1842–8.
35 Rhodes J, Margossian R, Sleeper LA, et al. Non-geometric echocardiographic indices of ventricular function in patients with a Fontan circulation. *J Am Soc Echocardiogr* 2011;**24**:1213–19.
36 Bellsham-Revell HR, Tibby SM, Bell AJ, et al. Tissue Doppler time intervals and derived indices in hypoplastic left heart syndrome. *Eur Heart J Cardiovasc Imaging* 2012;**13**:400–7.
37 Cheung MM, Smallhorn JF, Redington AN, Vogel M. The effects of changes in loading conditions and modulation of inotropic state on the myocardial performance index: comparison with conductance catheter measurements. *Eur Heart J* 2004;**25**:2238–42.
38 Friedberg MK, Silverman NH. The systolic to diastolic duration ratio in children with hypoplastic left heart syndrome: a novel Doppler index of right ventricular function. *J Am Soc Echocardiogr* 2007;**20**:749–55.
39 Sarnari R, Kamal RY, Friedberg MK, Silverman NH. Doppler assessment of the ratio of the systolic to diastolic duration in normal children: relation to heart rate, age and body surface area. *J Am Soc Echocardiogr* 2009;**22**:928–32.
40 Cordina R, Ministeri M, Babu-Narayan SV, et al. Evaluation of the relationship between ventricular end-diastolic pressure and echocardiographic measures of diastolic function in adults with a Fontan circulation. *Int J Cardiol* 2018;**259**:71–5.
41 Cordina R, von Klemperer K, Kempny A, et al. Echocardiographic predictors of mortality in adults with a Fontan circulation. *JACC Cardiovasc Imaging* 2017;**10**:212–13.
42 Friedberg MK, Mertens L. Deformation imaging in selected congenital heart disease: is it evolving to clinical use? *J Am Soc Echocardiogr* 2012;**25**:919–31.
43 Singh GK, Cupps B, Pasque M, Woodard PK, Holland MR, Ludomirsky A. Accuracy and reproducibility of strain by speckle tracking in pediatric subjects with normal heart and single ventricular physiology: a two-dimensional speckle-tracking echocardiography and magnetic resonance imaging correlative study. *J Am Soc Echocardiogr* 2010;**23**:1143–52.
44 Lopez C, Mertens L, Dragulescu A, et al. Strain and rotational mechanics in children with single left ventricles after Fontan. *J Am Soc Echocardiogr* 2018;**31**:1297–306.
45 Ghelani SJ, Harrild DM, Gauvreau K, Geva T, Rathod RH. Echocardiography and magnetic resonance imaging based strain analysis of functional single ventricles: a study of intra- and intermodality reproducibility. *Int J Cardiovasc Imaging* 2016;**32**:1113–20.
46 Cheung YF, Penny DJ, Redington AN. Serial assessment of left ventricular diastolic function after Fontan procedure. *Heart* 2000;**83**:420–4.
47 Rosner A, Khalapyan T, Dalen H, McElhinney DB, Friedberg MK, Lui GK. Classic-pattern dyssynchrony in adolescents and adults with a Fontan circulation. *J Am Soc Echocardiogr* 2018;**31**:211–19.
48 Khoo NS, Smallhorn JF, Kaneko S, Myers K, Kutty S, Tham EB. Novel insights into RV adaptation and function in hypoplastic left heart syndrome between the first 2 stages of surgical palliation. *JACC Cardiovasc Imaging* 2011;**4**:128–37.
49 Friedberg MK, Silverman NH, Dubin AM, Rosenthal DN. Right ventricular mechanical dyssynchrony in children with hypoplastic left heart syndrome. *J Am Soc Echocardiogr* 2007;**20**:1073–9.